ELSEVIER

Journal of Nuclear Materials 241–243 (1997) 559–563

journal of nuclear materials

SOL plasma profiles under radiative and detached divertor conditions in JT-60U

N. Asakura *, Y. Koide, K. Itami, N. Hosogane, K. Shimizu, S. Tsuji-Iio [1], S. Sakurai, A. Sakasai

Naka Fusion Research Establishment, Japan Atomic Energy Research Institute, Naka-gun, Ibaraki-ken 311-01, Japan

Abstract

Radial profiles of electron density $n_{e,mid}$, temperature $T_{e,mid}$, and ion temperature $T_{i,mid}$ in the scrape-off layer (SOL) were investigated under radiative and detached divertor conditions in L-mode discharges. Since the ratio of $T_{i,mid}/T_{e,mid}$ is about 3, the ion pressure is dominant at the midplane, and plays an important role in the pressure balance between the midplane and the divertor targets. Effect of the connection length on the decay lengths of $n_{e,mid}$ and $T_{e,mid}$, λ_{T_e} and λ_{n_e}, was determined in two SOL regions. At the same time, λ_{T_i} was compared to λ_{T_e} and λ_{n_e}. λ_{n_e}, λ_{T_e} and λ_{T_i} increase with the connection length. During the X-point MARFE, λ_{T_e}, λ_{n_e} and λ_{T_i} increase substantially with a reduction in $T_{e,mid}$, $T_{i,mid}$ and $n_{e,mid}$ at the plasma edge and in the first SOL, due to the penetration of the maximum radiation region into the main plasma near the X-point.

Keywords: JT-60U; SOL plasma; Detached plasma; Langmuir probe

1. Introduction

The radiated power is enhanced in high density discharges when a MARFE appears in the vicinity of the divertor X-point. This causes a reduction of the peak heat flux to the target and the plasma momentum detachment along the magnetic field line [1]. The concept of the plasma detachment is of great practical importance to the design of the ITER divertor. It is reported that the characteristic length of the radial profile (e-folding length) at the upstream SOL increases dramatically with a decrease in the edge electron temperature associated with the growth of the 'X-point MARFE' [2,3]. Under radiative and detached divertor conditions, the heat and particle transport in the SOL is modified by the location and size of the intense radiation region [4]. The first objective of this paper is to experimentally determine the temperature and density profiles with the radial resolution of a millimeter in order to understand the mechanism for the SOL plasma broadening. In this paper, I_p and B_t dependencies of the profiles are emphasized.

Ions carry the plasma momentum along the field line to the target, where it can be lost due to charge exchange or elastic collision with recycled neutrals in the X-point and divertor region. However, there have been few experimental results of the ion diffusion process and pressure balance between the midplane SOL and divertor plasmas [5,6]. The second objective is to investigate the pressure balance along the field line and the radial transport of the ions.

2. SOL profile measurement

Experiments were performed in high density L-mode discharges with $p_{NBI} = 4$ MW. Line-averaged density $\bar{n}_e$ was increased on a shot-to-shot basis, using feedback control of deuterium gas puffing to keep $\bar{n}_e$ at a constant level during the probe measurement. Profiles were measured in high safety-factor discharges ($q_{eff} = 7.2$–7.7, $I_p = 1.2$ MA, $B_t = 3.5$–4 T), and two combinations of I_p and

* Corresponding author. Tel.: +81-29 270 7341; fax: +81-29 270 7419; e-mail: asakura@expert1.naka.jaeri.go.jp.

[1] Present address: Research Laboratory for Nuclear Reactors, Tokyo Institute of Technology, Tokyo, Japan.

PII S0022-3115(96)00564-8

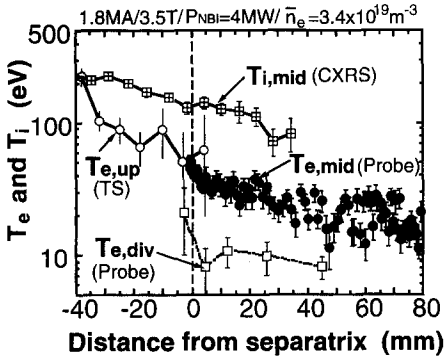

Fig. 1. Profiles of $T_{e,mid}$, $T_{e,up}$, $T_{i,mid}$ and the outer $T_{e,div}$ as measured with a reciprocating Langmuir probe, Thomson scattering (TS) system, CXRS and target Langmuir probe array, mapped on the midplane radius, represented by closed circles, open circles, crossed-squares, open squares. $\bar{n}_e = 3.4 \times 10^{19}$ m^{-3}, where a MARFE appears over the X-point.

B_t (I_p/B_t = 1.2 MA/2.1 T and 1.8 MA/3.5 T) are chosen for the low-q_{eff} discharges (q_{eff} = 4.3–4.7).

Electron temperature, $T_{e,mid}$, and density, $n_{e,mid}$, profiles are measured with a fast reciprocating Langmuir probe system [7] installed at the midplane with a spatial resolution of 1–2 mm. The double probe method is used to derive $T_{e,mid}$ and $n_{e,mid}$. Values of $T_{e,mid}$ and $n_{e,mid}$ at the separatrix are compared to those obtained by the Thomson scattering (TS) system, $T_{e,up}$ and $n_{e,up}$, viewing the upper edge of the plasma vertically. $T_{e,mid}$ and $n_{e,mid}$ are in a good agreement with $T_{e,up}$ and $n_{e,up}$, respectively within the relatively large error bars of the TS measurement at the edge region (30–50%).

Fifteen dome-type Langmuir probes mounted at the divertor target measure the electron temperature, $T_{e,div}$, and density, $n_{e,div}$, with a spatial resolution of 2.5–5 cm at the target [8]. Separation of adjacent magnetic flux surfaces at the target is about 3–4 times larger than that at the outer midplane.

The ion temperature profiles in the edge plasma (at about 1 m above the midplane), $T_{i,mid}$ are measured with charge exchange recombination spectroscopy system (CXRS), using a carbon charge exchange line of C^{6+} (n = 8–7) at 529.2 nm. A best spatial resolution of 6–7 mm is obtained since the scope (32 fiber array) views are perpendicular to the neutral beam line on the poloidal cross-section.

Fig. 1 shows the profiles of $T_{e,mid}$, $T_{i,mid}$ and the outer $T_{e,div}$ at high density ($\bar{n}_e = 3.4 \times 10^{19}$ m^{-3}), where a MARFE appears outside the X-point for the ion ∇B drift direction towards the target [9]. All profiles are mapped to the midplane using the equilibrium calculation. The accuracy of the magnetic separatrix position is about 5 mm. $T_{e,div}$ is lower than $T_{e,mid}$, particularly with increasing $\bar{n}_e$, and $T_{i,mid}$, $T_{e,mid}$ and $T_{e,div}$ = 130, 42 and 8 eV are observed at the separatrix, respectively. A maximum density of $n_{e,div} = 4 \times 10^{19}$ m^{-3} is observed at the second divertor probe outside the separatrix. On the other hand, $n_{e,div}$ at the first divertor probe outside the separatrix is 1×10^{19} m^{-3}, which indicates that the plasma detachment occurs first close to the divertor separatrix. A width of the region corresponds to a size of 10 mm in the midplane radius.

3. Plasma pressure balance along the field line

In the plasma edge and SOL region, $T_{i,mid}$ is higher than $T_{e,mid}$ as shown in Fig. 1. Fig. 2 represents the ratio of $T_{i,mid}$ to $T_{e,mid}$ at 2–4 mm outside the separatrix for the medium and high density discharges with different q_{eff}. The maximum density, at which the X-point MARFE appears, is limited by the gas puff rate not due to the high density disruption. The ratio ranges between 2.5 and 3.8, while both $T_{i,mid}$ and $T_{e,mid}$ are reduced from 300 to 65 eV and from 80 to 22 eV with increasing $\bar{n}_e$, respectively. Parallel ion energy confinement time (i.e. ion transit time), τ^i_{par}, is given by $3n_iT_iL_c/2q^i_{\|}$, where $q^i_{\|}$ is the parallel ion heat flux density, L_c connection length, and $n_i = n_e$ is assumed. Under the above condition of the SOL plasma, ions are thermally decoupled from electrons: τ^i_{par} ranges between 0.1 and 0.5 ms, which is shorter than the electron–ion thermalization time, τ^{i-e}_{th}, of 1–10 ms. Thus, it is expected that $T_{i,mid}$ is higher than $T_{e,mid}$ due to the low parallel thermal conductivity of ion by a factor of $(m_i/m_e))^{1/2} \sim 60$ for deuterium plasma. The measured value of $T_{i,mid}/T_{e,mid} \sim 3$ at the separatrix is consistent with $T_{i,mid}/T_{e,mid} = (m_i/m_e)^{1/9} \sim 2.5$, which is predicted by the SOL/divertor two-point model assuming cross-field heat conductivity and the power into the SOL, P_{SOL}, are the same for the ion and electron [6].

As a result, ion pressure is generally dominant compared to electron pressure in the SOL and edge plasmas. Fig. 3 shows the ratio of the static and dynamic pressure at

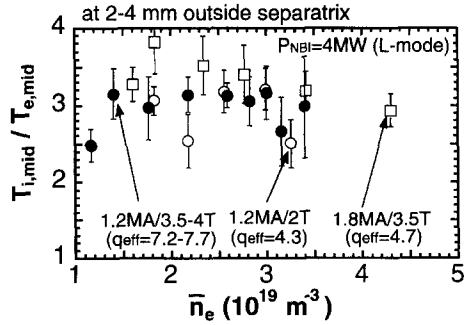

Fig. 2. Ratio of $T_{i,mid}$ to $T_{e,mid}$ at the separatrix at medium and high densities: Closed circles, open circles and squares correspond to the discharge with $I_p/B_t/q_{eff}$ = 1.2 MA/3.5–4 T/7.2–7.7, 1.2 MA/2.1 T/4.3, and 1.8 MA/3.5 T/4.7, respectively. One or two data at the high density for each q_{eff} are measured during the X-point MARFE.

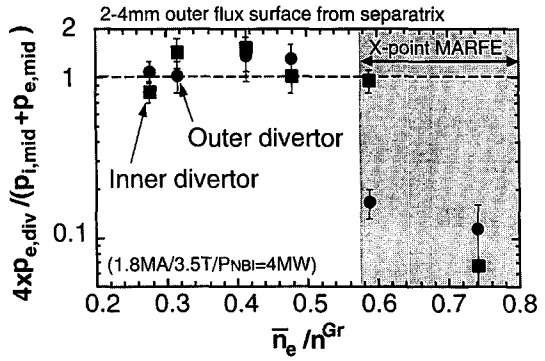

Fig. 3. The ratio of the static and dynamic total pressure at the inner (squares) and outer (circles) divertor targets to total plasma pressure ($p_{mid} = p_{i,mid} + p_{e,mid}$) at the midplane separatrix. Here, total divertor plasma pressure is given by $2\times(p_{i,div} + p_{e,div}) = 4 \times p_{e,div}$, assuming $T_{i,div} = T_{e,div}$ and Mach number $M = 1$. The value of 1 corresponds to the total pressure balanced between the midplane and the divertor.

the inner and outer divertor separatrix to the total plasma pressure ($p_{i,mid} + p_{e,mid}$) at the midplane separatrix as a function of line-averaged electron density normalized by the 'Greenwald density' ($n^{Gr} \equiv I_p/\pi a^2$, where a is a midplane minor radius). Here, the former is given by $2(p_{i,div} + p_{e,div}) = 4p_{e,div}$, where $T_{i,div} = T_{e,div}$ and Mach number $M = 1$ at the target are assumed. The assumption of $T_{i,div} = T_{e,div}$ is feasible at the high density, since τ_{th}^{i-e} near the divertor target is decreased by the factor of 5–50 compared with that at midplane. The ratio of 1 corresponds to total plasma pressure balanced between at the inner and outer divertor targets, and that at midplane. The result shows that the total plasma pressure balance is maintained along open field lines at $\bar{n}_e$ lower than the occurrence of an X-point MARFE. When the X-point MARFE occurs, however, the plasma pressure at the outer divertor is reduced by an order of magnitude. On the other hand, the plasma pressure at the inner target stays at a constant level, and finally decreases at still higher $\bar{n}_e$. The reduction in the plasma pressure is indicated by a reduction in the ion saturation current (ion flux), since $T_{e,div}$ is relatively constant (7–13 eV). The relatively high $T_{e,div}$ for the detached plasma is presumably caused by the probe measurement of the high energy electron tail rather than the Maxwellian distribution of the bulk electrons [6,10].

4. SOL profiles at high density

The time evolution of the $n_{e,mid}$ profile is shown in Fig. 4 at $\bar{n}_e = 1.9$, 2.8 and 4.3×10^{19} m^{-3}, which correspond to low and high recycling divertor conditions, and during the X-point MARFE, respectively. Two (i.e. first and second) SOL regions with different characteristic lengths are observed both in the $n_{e,mid}$ and $T_{e,mid}$ profiles.

4.1. $n_{e,mid}$ and $T_{e,mid}$ profiles in first SOL

The first SOL, where large fractions of the heat and particle fluxes are carried to the divertor along the field line, extends up to 10–15 mm outside the separatrix. The profile has a small e-folding length provided that the attached divertor condition is maintained; local e-folding lengths of $n_{e,mid}$ and $T_{e,mid}$ are $\lambda_{n_e} = 14$–17 mm, and $\lambda_{T_e} = 22$–25 mm for $I_p = 1.8$ MA, $B_t = 3.5$ T (the safety factor, q_{eff} of 4.7). The values are approximately the same with increasing $\bar{n}_e$ or local density at the magnetic separatrix $n_{e,sep}$. Fig. 5 shows the local λ_{n_e} and $n_{e,sep}$ as a function of $T_{e,sep}$. Both λ_{n_e} and λ_{T_e} are increased with q_{eff}. A regression analysis for $T_{e,sep} \geq 45$ eV suggests that $\lambda_{n_e} \propto q_{eff}^{\alpha} T_{e,sep}^{\beta}$, where $\alpha = 0.85 \pm 0.12$ and $\beta = 0.23 \pm 0.15$, and $\lambda_{T_e} \propto q_{eff}^{\alpha} T_{e,sep}^{\beta}$, where $\alpha = 0.5 \pm 0.1$ and $\beta = -0.3 \pm 0.2$ and λ_{T_e} is by a factor of 1.5–2 larger than λ_{n_e}. The decay lengths increase strongly with the connection length. Here, the q-dependencies of λ_{n_e} and λ_{T_e} with varying I_p are weaker than those with varying B_t. The values of α and β for λ_{n_e} are close to those obtained in ASDEX [2].

When the X-point MARFE appears, $n_{e,sep}$ does not increase and then decreases as $T_{e,sep}$ decreases in Fig. 5(b). At the same time, both λ_{n_e} and λ_{T_e} are increased substantially. At the occurrence of the X-point MARFE, the fraction of the radiation power in the outboard divertor increases up to 75–80% of power flow to the outer divertor fan, and $T_{e,sep}$ at the midplane is between 40 and 45 eV. The critical $T_{e,sep}$ is the same for the discharges with different connection lengths. This is because the radiation region near the X-point enters into closed magnetic flux surface, causing the reduction of $T_{e,mid}$ at the upstream edge plasma as $\bar{n}_e$ is increased further. Note that the maximum $n_{e,sep}$ given near the MARFE onset increases with I_p rather than the connection length. The

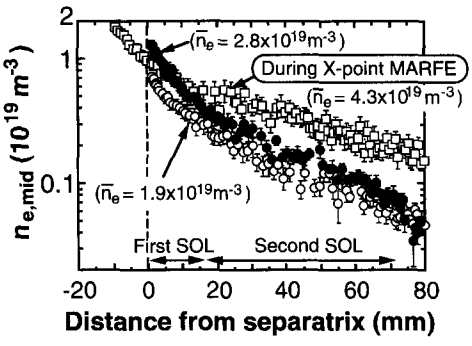

Fig. 4. Density profiles at the midplane: under the attached divertor conditions (open and closed circles) and during the X-point MARFE (squares), which correspond to $\bar{n}_e = 1.9$, 2.8 and 4.3×10^{19} m^{-3}, respectively. $I_p = 1.8$ MA, $B_t = 3.5$ T with $p_{NBI} = 4$ MW L-mode. First and second SOL regions having different e-folding lengths are observed.

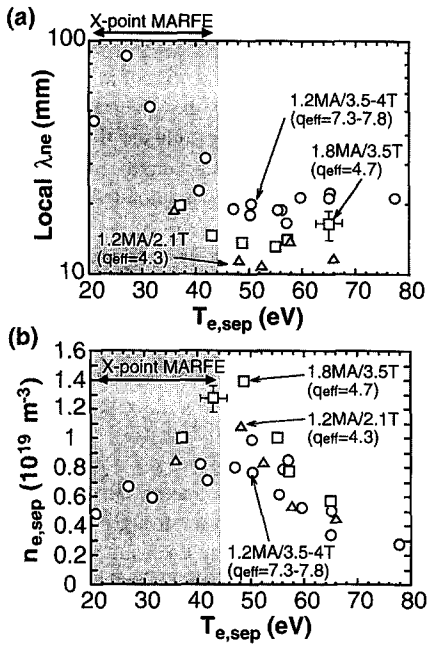

Fig. 5. (a) the local e-folding length of $n_{e,mid}$ in the first SOL and (b) $n_{e,sep}$ as a function of $T_{e,sep}$: circles, triangles and squares correspond to the discharges with $I_p/B_t/q_{eff} = 1.2$ MA/3.5–4 T/7.2–7.7, 1.2 MA/2.1 T/4.3, and 1.8 MA/3.5 T/4.7, respectively.

particle and energy confinement of the edge plasma is improved at high density with increasing I_p.

The edge pedestal of $n_{e,up}$, $T_{e,up}$, and $T_{i,mid}$ profiles, measured with the Thomson scattering system and CXRS system, moves inward from $r/a = 0.98$ to 0.90 during the X-point MARFE; i.e. $n_{e,up}$ $T_{e,up}$ and $T_{i,mid}$, in particular, inside the separatrix is reduced significantly. At the same time, $n_{e,up}$ profile becomes peaked. The results indicate that the MARFE extends into the confined plasma, resulting in an increase in the radiation power not only near the divertor X-point region but also at the main plasma edge, and in the degradation of the edge confinement.

4.2. Electron and ion profiles in second SOL

The second SOL region exists in the region from 10–15 mm to 80–100 mm at the midplane as shown in Fig. 4. Local decay length in the second SOL is deduced by fitting an exponential function to the profile in the second SOL region. Although $n_{e,mid}$ and $T_{e,mid}$ are by a factor of 2–3 smaller than those at the separatrix, Fig. 6 shows that λ_{n_e} (30–60 mm) and λ_{T_e} (60–130 mm) in the second SOL are by a factor of 2–3 larger than those in the first SOL. This increase is associated with a reduction in $T_{e,sep}$ (i.e. an increase in $\bar{n}_e$). The decay length of $T_{i,mid}$ profile can be fitted by an exponential function over the entire radial region extending 50–60 mm outside the separatrix, which includes the first and second SOLs of the electron temperature profiles. The $T_{i,mid}$ profile at the first SOL may not be resolved by the large spatial resolution of 6–7 mm. The e-folding length of $T_{i,mid}$, λ_{T_i}, is by a factor of 2.5–3 larger than λ_{T_e} at the first SOL. Thus, the ratio, $T_{i,mid}/T_{e,mid}$, is 3.5–4.5 at the outer flux surfaces, which is larger than 3 at the separatrix. λ_{T_i} is increased with q_{eff} strongly compared to that of $T_{e,mid}$ in the first SOL; $\lambda_{T_i} \propto q_{eff}^{\alpha} T_{i,sep}^{\beta}$, where $\alpha = 0.8 \pm 0.2$ and $\beta = -0.3 \pm 0.2$ for $T_{e,sep} \geq 45$ eV. The results are consistent with the prediction of the SOL two-point model, i.e. $\lambda_{T_i}/\lambda_{T_e} = (m_i/m_e)^{1/9} \sim 2.5$, due to the low parallel thermal conductivity of ion. A good correlation between λ_{T_i}, λ_{T_e} and λ_{n_e} is found in the second SOL; $\lambda_{T_e} \sim 2\lambda_{n_e}$ and $\lambda_{T_i} \sim 1.6\lambda_{n_e}$. This suggests that radial convection may contribute to the cross-field heat transport in this region.

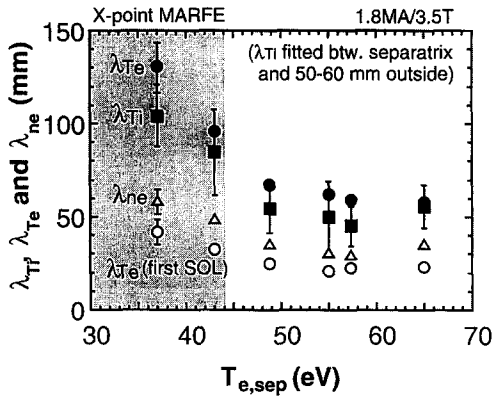

Fig. 6. e-folding lengths in the second SOL. λ_{n_e} (triangles), λ_{T_e} (closed circles), and λ_{T_i} (squares) as a function of $\bar{n}_e$, where $I_p/B_t = 1.8$ MA/3.5 T. Here, λ_{T_i} is fitted by an exponential function between the separatrix and 50–60 mm outside. Open circles represent λ_{T_e} at the first SOL.

During the X-point MARFE, $n_{e,mid}$ and $T_{e,mid}$ in the second SOL stay at relatively constant levels: $n_{e,mid}$ of $(2–4) \times 10^{18}$ m^{-3} and $T_{e,mid}$ of 10–15 eV, while $n_{e,mid}$

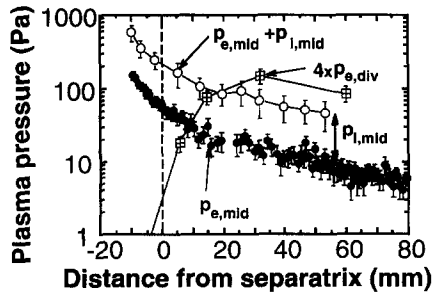

Fig. 7. Electron and total (electron plus ion) pressures at the midplane, and total (static and dynamic) pressure at the outer divertor are shown by open circles, closed circles and squares, respectively. Profiles are measured simultaneously during the X-point MARFE at $\bar{n}_e = 4.3 \times 10^{19}$ m^{-3}.

and $T_{e,mid}$ in the first SOL are decreased. Thus, all the decay lengths in the SOL increase substantially. Not only the broadening of the decay length but also the transport of the plasma momentum is modified in the divertor. Fig. 7 shows that the total (static and dynamic) plasma pressure in the second SOL at the outer target is larger than $p_{i,mid} + p_{e,mid}$. This suggests that the plasma gains momentum in the second SOL, while the divertor plasma detachment proceeds at the first SOL. The particle recycling is enhanced at the outboard target, and the decay length of the SOL profile increases significantly. Under the radiative divertor condition, ionization mean-free-path of a thermal neutral of energy 50 eV is estimated to be 20 cm at the relatively high density divertor plasma of $n_e = 2 \times 10^{19}$ m^{-3} and $T_e = 10$ eV. It is possible to cause re-ionization of a part of thermal neutrals within the broad SOL region. Enhancement of the convection loss, flow reversal or probe measurement of high energy electrons may be other candidates.

5. Conclusion

The radial profiles of $n_{e,mid}$, $T_{e,mid}$ and $T_{i,mid}$ in the SOL were investigated for the different I_p and B_t in the high density L-mode discharges. $T_{i,mid}$ is by a factor of 3 higher than $T_{e,mid}$, and the $T_{i,mid}$ profile extended to the outer flux surfaces; λ_{T_i} is by a factor of 2.5–3 larger than λ_{T_e} at the first SOL. Since ion pressure is dominant in the edge plasma and SOL, ions play a crucial role in the pressure balance in the SOL and divertor. The decay lengths of $n_{e,mid}$, $T_{e,mid}$ and $T_{i,mid}$ profiles, increase with the connection length. Since a MARFE enters closed magnetic flux surfaces near the X-point, those profiles becomes significantly flat in the SOL, when $n_{e,mid}$, $T_{e,mid}$ and $T_{i,mid}$ are reduced in the plasma edge (inside the separatrix and the first SOL).

Acknowledgements

The first author would like to thank Dr. M. Shimada and Dr. C.S. Pitcher for very useful comments.

References

[1] C.F. Matthews et al., J. Nucl. Mater. 220–222 (1995) 104.
[2] K. McCormick et al., J. Nucl. Mater. 196–198 (1992) 264.
[3] B. LaBombard et al., Phys. Plasmas 2 (1995) 2242.
[4] C.S. Pitcher et al., J. Nucl. Mater. 220–222 (1995) 213.
[5] T.W. Petrie et al., J. Nucl. Mater. 196–198 (1992) 848.
[6] C.S. Pitcher and P.C. Stangeby, Plasma Phys. Controlled Fusion, to be published.
[7] N. Asakura et al., Rev. Sci. Instrum. 66 (1995) 5428.
[8] N. Asakura et al., Nucl. Fusion 35 (1995) 381.
[9] N. Asakura et al., in: Plasma Physics and Controlled Nuclear Fusion Research, Proc. 15th Int. Conf. Seville, 1994, Vol. 1 (IAEA, Vienna, 1995) p. 515.
[10] A.A. Batishcheva et al., Proc. 5th Plasma Edge Theory Conf., Asilomar, 1995, Controlled Plasma Phys. 36 (1996), to be published.